Available online at www.sciencedirect.com
SCIENCE DIRECT®
Journal of Sound and Vibration 283 (2005) 573–588
JOURNAL OF SOUND AND VIBRATION
www.elsevier.com/locate/jsvi

On the spectral characteristics of a self-excited Rijke tube combustor—numerical simulation and experimental measurements

Prateep Chatterjee[a], Uri Vandsburger[a,*], William R. Saunders[a], Vivek K. Khanna[b], William T. Baumann[c]

[a]*Department of Mechanical Engineering, Virginia Polytechnic Institute and State University, Randolph Hall, Blacksburg, VA 24061-0238, USA*
[b]*Solar Turbines, 2200 Pacific Highway, San Diego, CA 92123, USA*
[c]*Department of Electrical Engineering, Virginia Polytechnic Institute and State University, Blacksburg, VA 24061, USA*

Received 16 June 2003; accepted 29 April 2004

Abstract

A computational fluid dynamics (CFD) study has been conducted to investigate the occurrence of combustion instabilities in a Rijke tube type of combustor. The purpose of the study has been to capture the reacting flow physics in the combustor using two-dimensional finite-volume solution of the conservation equations in order to predict the frequency and magnitude of the thermoacoustic instability. It has been observed from literature that past attempts at simulation of reacting flow inside Rijke tubes have not been successful at explaining the self-excited mechanism between unsteady heat release and acoustics. Instead, time-varying heat sources or instability triggering mechanisms (forced response) have been used. In the present study, time integration of the conservation equations enabled the capture of the self-excited three-quarter mode of the combustor. Results from associated experimental studies have been included to describe the acoustic signature of the combustor. Comparison between the computed and experimentally obtained results validate the theories proposed in an earlier study. The thermoacoustic instability frequency has been predicted at 190 Hz as compared to the experimental value of 182 Hz whereas the magnitude has been found to match the experimental value of 177 dB. The results confirm the ability of the CFD analysis

*Corresponding author. Tel.: +1-540-231-5882; fax: +1-540-231-9909.
E-mail address: uri@vt.edu (U. Vandsburger).

0022-460X/$ - see front matter
doi:10.1016/j.jsv.2004.04.019

in capturing the instability growth to a limit-cycle of pressure oscillation and its success in predicting the instability frequency as well as harmonics of the instability frequency.

1. Introduction

Stringent emissions standards imposed in recent years have led to the design and installation of lean, premixed gas turbine combustors. In these types of combustors thermoacoustic combustion instabilities occur at certain lean operating conditions. The occurrence of these thermoacoustic instabilities is characterized by large acoustic pressures (rms) inside the combustion chamber. Large fluctuating pressure (p') and unsteady heat release over a large area of the combustion chamber creates stresses that can lead to structural failure of the liner or other parts of the gas turbine. To be able to prevent the instabilities from happening or to control them, there is a need to understand the controlling mechanisms and to develop capabilities for prediction of the conditions under which they occur. The Rijke tube combustor provides an elementary example of thermoacoustic oscillation with heat release from the flame (which is anchored on a grid inside the tube) as a source of excitation. There is a large amount of information that resides in the spectral representations of any dynamic system response for both linear and nonlinear systems. The information supports descriptions of physical phenomena responsible for unique spectral features. Therefore, by analyzing the Rijke tube it will be possible to discern the details of the thermoacoustic pressure signatures for both dynamic modeling and system monitoring in any combustor system. There are some important limitations associated with the study of thermoacoustic instabilities in Rijke tubes versus real, full-scale combustors. The fluid dynamic coupling in the Rijke tube is not of importance, as there are no vortical structures in the flow (because of the laminar flow regime selected) that can cause periodic heat release. This simplifies the investigation of features that are the focus of this present study. Specifically, the Rijke tube combustor was intentionally selected to eliminate coupling between thermoacoustic instabilities and flow instabilities.

Both experimental studies and analytical modeling of Rijke tubes have been reported previously by several researchers [1–3]. A one-dimensional initial value problem approach was chosen by Nark and Hardin [4] whereas Yoon et al. [5] used modal analysis to produce a linear velocity sensitive thermoacoustic response model. Recently, Nord [6] conducted both experimental and theoretical studies on a tube combustor similar to a Rijke tube and proposed three distinct mechanisms affecting the acoustic pressure in the tube. The three mechanisms are: a main thermoacoustic instability in accordance to the Rayleigh criterion [7]; a vibrating flame instability where the flame sheet exhibits mode shapes; and a pulsating flame instability driven by thermodiffusive heat losses to the flame stabilizer.

Numerical modeling, especially computational fluid dynamics (CFD) based modeling, has been reported more recently. Yan [8] used second-order accurate schemes to simulate two-dimensional self-excited oscillating flows in a Rijke tube configuration. The combustion process was substituted by the presence of a heat source, in effect eliminating the possibility of capturing the thermo-diffusive instability (the pulsating flame instability mentioned above) which is due to the heat transfer interaction between the flame stabilizer and the flame. Though the authors were

studying a self-excited system, a sinusoidally time-varying energy release from the heat source was imposed. A range of forcing frequencies were chosen to determine the optimal frequency (matching the natural frequency of the structure) of the simulation through pressure wave numbers.

Another similar one-dimensional study using a heat source and heat sink pair was conducted by Ishii et al. [9]. A steady heat supply was maintained to the heat source and the heat flux into the fluid (assumed to be an ideal gas) was allowed to fluctuate because of the velocity variation. This variation was explained with a hypothesis that due to the steep temperature gradient between the heat source and the heat sink, thermal energy was transformed into mechanical energy (heat-induced vibration). Such a phenomena is different from thermoacoustic driving mechanism and hence the model cannot be of help in understanding combustion instabilities. Entezam et al. [10] have used FLOW-3D software [11] to simulate flow in a Rijke tube. A solid porous obstacle was used as the heat source with a step-input chosen for the heat release. The authors have used dimensional analysis [12] to create a similarity parameter relating the oscillating heat flux to pressure, velocity and a characteristic length.

In a recent study, Hantschk and Vortmeyer [13] applied the commercial CFD code FLUENT 4.4.4 [14] to simulate self-excited thermoacoustic oscillations in a Rijke tube which resulted from an interaction between the heat transferred to the fluid from hot wires and the acoustics of the geometry. Two different kinds of Rijke tubes were modeled—open–open and closed–open tubes. The authors used an initial pressure oscillation to initiate the self-excited oscillation process in the tube. In their analysis, although higher harmonics of the instability frequency were observed, detailed analysis of the pressure power spectrum was not carried out to investigate the nonlinear coupling between heat release rate and the tube acoustics. The authors mention the importance of modeling actual combustion systems [15] in understanding thermoacoustic instabilities and the importance of using a Rijke tube burner in such studies.

To completely understand thermoacoustic instabilities occurring in combustion systems, combustion modeling needs to be incorporated in the model. Perhaps the most comprehensive CFD study of thermoacoustic instabilities in Rijke tubes implementing combustion modeling till date has been conducted by Sangyeon et al. [16]. Attention was given to the fundamental mode in the tube rather than the higher modes of oscillation. Single-step propane–air global reaction mechanism to simulate chemical reaction and k–ε turbulence modeling were incorporated using the KIVA-II code [17]. The honeycomb flame-holder present in the associated experimental study was not considered for the simulation and forced oscillation was used as a triggering mechanism to simulate unsteady behavior of the flow.

The present study aims at capturing the fundamental frequency of the thermoacoustic instability observed in an experimental study conducted on a Rijke tube combustor along with capturing other features of the power spectrum like the thermodiffusive instability that was also observed in the experimental study. The modeling effort is directed toward capturing the physics of the coupling mechanism between acoustics and the unsteady heat release mechanism from the flame. The Navier–Stokes equations were solved using accurate numerical integration and time-marching schemes, and finite rate chemistry. FLUENT 5.1-5.3 [14] CFD software was used and a two-dimensional simplification of the Rijke tube experimental setup [18] was considered for the study. A multi-passage honeycomb flame holder was included in the grid to capture the pulsating flame instability. Instead of attempting to model the heat source (e.g. imposed time-varying heat

source), the aim has been to capture the flame–honeycomb heat transfer coupling process which is critical for proper presentation of physics. This inclusion sets apart the present study from the attempts carried out earlier because the flame–honeycomb coupling is modeled accurately instead of considering time-varying heat sources or artificially created temperature gradients.

2. Accompanying experimental study

2.1. Experimental setup

A very simple combustion device was selected to facilitate initial studies of thermoacoustic instabilities by the Virginia Active Combustion Control Group (VACCG) at Virginia Tech. A carbon steel tube combustor, as seen in Fig. 1, 1.524 m in length and 7.239 cm inner diameter was built [18]. Premixed methane–air mixture coming from a gas mixer was fed into the bottom part of the combustor through copper tubes with small holes drilled in the cylindrical shaper tubes. The main goal of the experimental study was to provide accurate acoustic pressure measurements

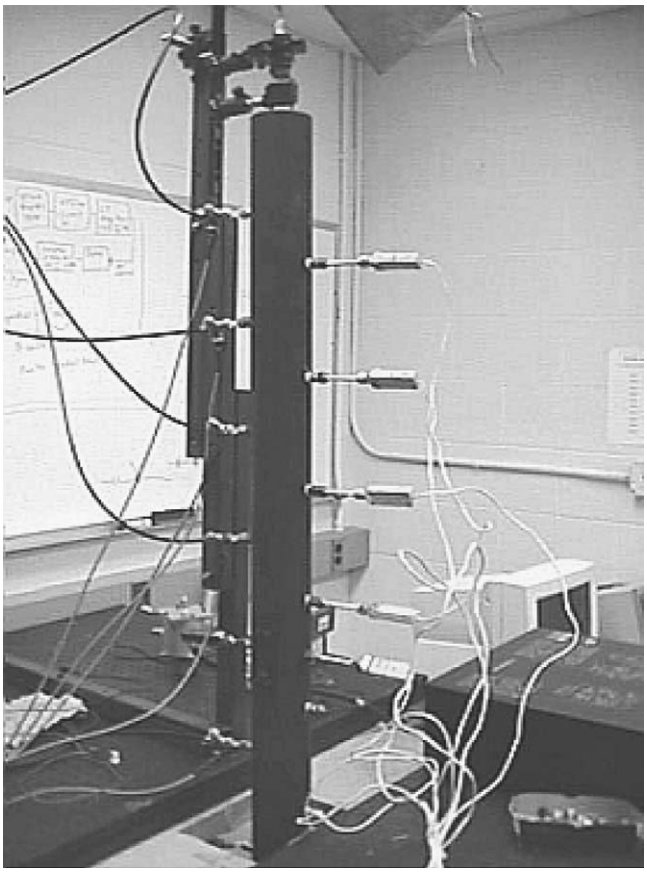

Fig. 1. The Rijke tube combustor—present study.

toward modeling efforts—identification of reduced-order modeling schemes: energy methods relying on Rayleigh's integral criteria, analytical description of conservation equations, and numerical solutions. The present CFD study was conducted to examine and validate the physics observed from the experiments.

The flame stabilizer (ceramic honeycomb) was mounted half-way from the bottom of the tube combustor for excitation of the second acoustic mode. The tube combustor is similar to a Rijke tube except that the boundary conditions are closed–open versus open–open for a Rijke tube. According to the Rayleigh criterion [7] this leads to a thermoacoustic instability of the second acoustic mode when the flame is placed at the middle of the tube (for the closed–open tube).

2.2. *Acoustic signature of the combustor*

The acoustic pressure signature exhibits useful information of the system that can be used in identifying reduced-order schemes which provide adequate prediction capabilities for the occurrence and control of thermoacoustic instabilities. In the pressure spectrum shown in Fig. 2 several regions can be identified:

(1) Around 180 Hz the fundamental frequency can be observed. In this case, the second acoustic mode of the combustor goes unstable in agreement with the Rayleigh criterion. The harmonics of the limit-cycle are also visible in the spectrum.
(2) A peak can be observed at half the limit-cycle frequency. The hypothesis is that an oscillation of the flame sheet occurs with double the period of the forcing function which in our case is because of acceleration of the gas column surrounding the flame [19].
(3) A low-frequency peak called the *pulsating flame instability*, between 10 and 20 Hz is also visible (magnified in Fig. 4). This subsonic frequency is responsible for modulating other peaks in the spectrum.

The following sub-sections include the description of the different features mentioned above.

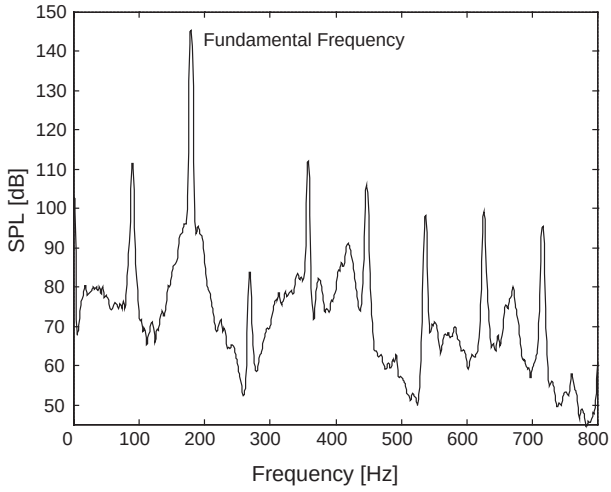

Fig. 2. Pressure power spectrum from experiment.

2.2.1. Subharmonic response

Markstein [19], using perturbation methods, modeled the distortion of the flame front as a second-order oscillator. He showed that there is a region of instability which renders flame oscillations at half the frequency of the parametric (acoustic) forcing. It is possible that such a flame instability drives the acoustics, leading to subharmonic resonances of pressure. When the flame sheet oscillates, the flame surface area changes and since the heat release is proportional to the flame surface area, the heat release also oscillates. In addition, as the flame oscillates, the heat loss to the flame stabilizer and the combustor walls changes which leads to a change in the net heat input to the gas. This change in heat release couples with the acoustic particle velocity and therefore we see a subharmonic peak (Fig. 3) at half the limit-cycle frequency in the pressure power spectrum.

To determine if this feature in the tube combustor is the same as Markstein described, experiments were conducted to dampen the thermoacoustic instability as well as shift the frequency of the instability to check the effect on subharmonic response magnitude and frequency. It was noted that the level of the thermoacoustic instability affects the subharmonic instability. For a certain frequency of the limit-cycle, there is a threshold minimum amplitude that the limit-cycle must have to drive the subharmonic instability. This minimum amplitude value changes according to the change in the frequency of limit-cycle and the flame-sheet seems to have preferred frequencies which can be seen as resonances of the flame (mode shapes).

2.2.2. Pulsating instability

At higher equivalence ratios ($\phi > 0.65$) the thermoacoustic instability shows evidence of amplitude modulation. The characteristic sidebands are evident throughout the spectrum but are especially obvious around the subharmonic and fundamental limit-cycle frequencies. This energy is related to a 'pulsating instability' as defined by Margolis [20] and is a type of thermal-diffusive

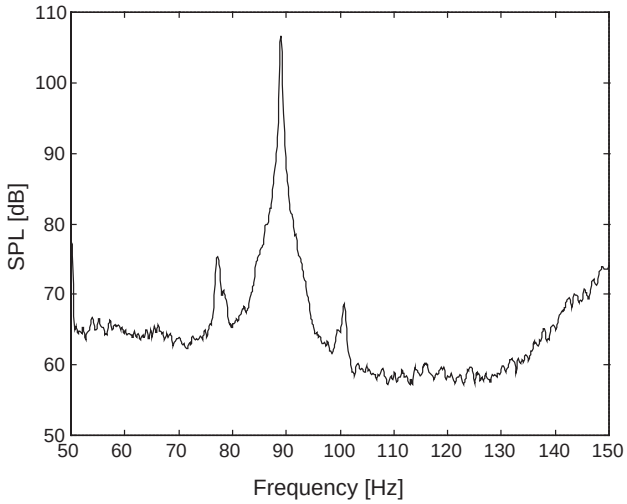

Fig. 3. Pressure power spectrum showing the subharmonic response.

instability that promotes the flame-sheet to move toward and away from the burner periodically, thereby modulating the overall rate of change of heat release to the acoustic mode.

This subharmonic response (Fig. 4) of the flame is observed to cause an amplitude modulation of the limit-cycle, the subharmonic response and the harmonics. Fig. 5 shows the sidebands as a consequence of amplitude modulation (shown as 'AM' in the figure). The frequency range observed in the tube combustor is in the same range as described in the Margolis theory [20]. There are numerous other effects which can be observed in the response of the self-excited combustion process. In effect, the experimental study showed that there is coupling between flame instabilities and thermoacoustic instabilities.

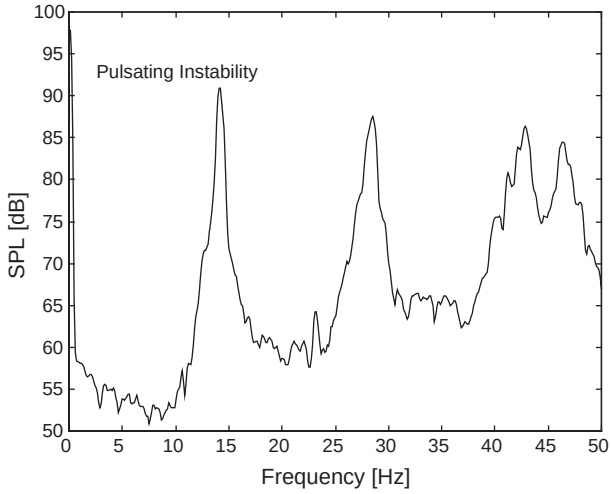

Fig. 4. Pressure power spectrum of pulsating flame instability (—, $\phi = 0.58$).

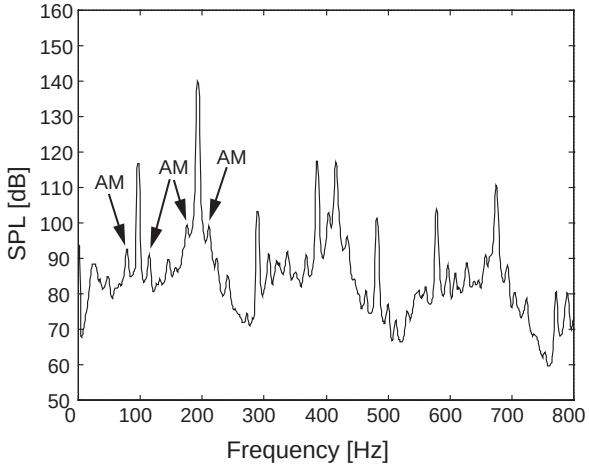

Fig. 5. Pressure power spectrum showing amplitude modulation (AM).

3. Computational model

A two-dimensional representation of the Rijke tube apparatus has been used for simulating the reacting flow. The computational geometry used in the solution process is illustrated in Fig. 6 with the thicker lines, and the actual internal geometry of the tube is shown by the thinner lines.

3.1. Grid generation

A hybrid—structured (quadrilateral) and unstructured (triangular)—grid was generated using the GAMBIT 1.0 [14]. The upstream portion of the grid was kept structured, followed by an unstructured grid just upstream of the honeycomb. A similar structure of the grid was imposed downstream of the honeycomb. This transition was necessary to make the grid size outside the honeycomb independent of the grid inside the honeycomb. The grid near the flame location (downstream of the honeycomb) is shown in Fig. 7 and the transition from quadrilateral grid

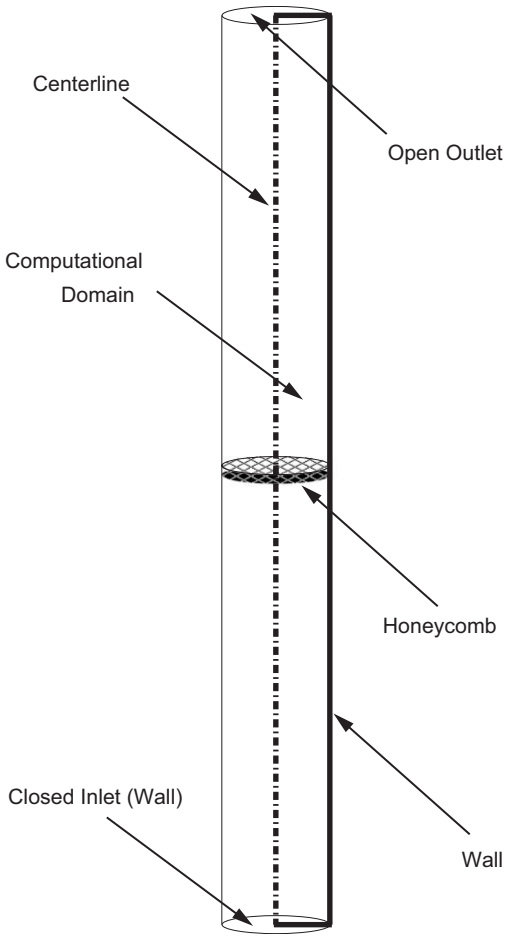

Fig. 6. Rijke tube computational geometry (not to scale).

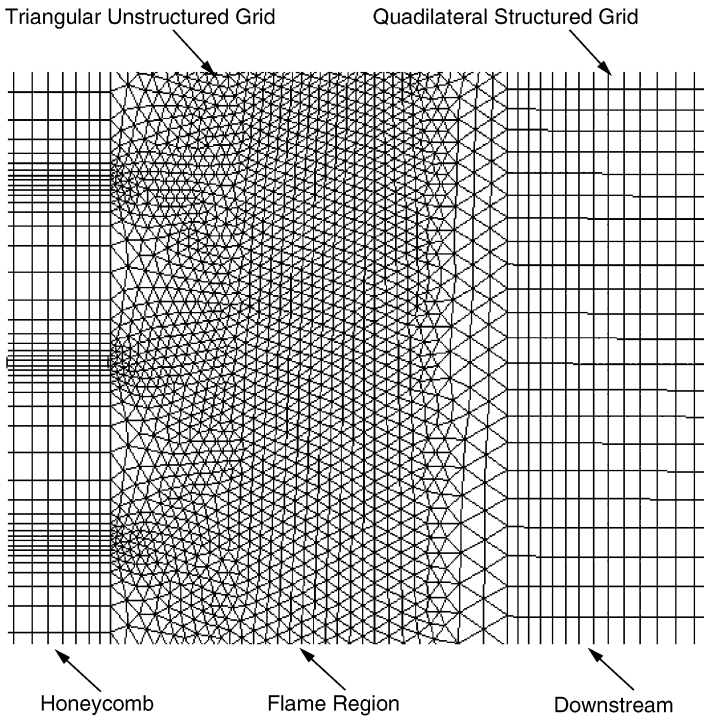

Fig. 7. Grid inside the honeycomb passages, flame region and downstream.

inside the honeycomb to triangular in the flame region and subsequently back to quadrilateral grid further downstream is illustrated.

3.2. Numerical method

Two-dimensional unsteady Navier–Stokes equations along with the continuity equation, energy equation and species equations have been solved using the Fluent 5.1-5.3 segregated solver (FLUENT/UNS [21]). Mixing and transport of species was modeled by solving conservation equations describing convection, diffusion, and reaction sources for each component species. A single-step mechanism has been used for the global reaction of methane and air [22]. For the species properties, different formulations in FLUENT were chosen.

A first-order implicit formulation in time along with second-order accurate spatial discretization were used in the solution process. A time step of 1.22×10^{-5} s was chosen to capture the time-varying pressure fluctuations. The small time step chosen also eliminated any effects of the first-order formulation in time over the overall order of the numerical scheme. A second-order accurate scheme was used for pressure interpolation. Second-order accurate upwind schemes have been used for momentum, species and in the energy equation whereas a first-order accurate scheme was used for calculating density. A pressure-implicit with splitting of operators

scheme has been used for pressure–velocity coupling. Global convergence criteria were set at 10^{-4} for momentum and continuity residuals and 10^{-6} for energy and species concentrations.

3.3. Boundary conditions

The closed-bottom acoustic inlet boundary condition was implemented by using a uniform and steady inlet velocity profile. This profile ensured an acoustically closed inlet ($u' = 0$). The mean velocity as well as methane and oxygen mass fractions were specified at the bottom inlet of the combustor. The density of the incoming mixture was determined by the Gibbs–Dalton law (mixture of ideal gases). A part-reflecting boundary condition was applied at the outlet where the pressure was 1 atm, thus implementing the open acoustic boundary condition ($p' = 0$). The walls were treated as convective boundaries where an outside (ambient air side) heat transfer coefficient was specified.

4. Results and discussion

The primary objective of this study was to develop a two-dimensional CFD model enabling accurate modeling of the thermoacoustic instability occurring in the combustor. To achieve the objective it was required that the fundamental frequency of the thermoacoustic oscillation be captured with reasonable accuracy. It is demonstrated in this section that the fundamental frequency of oscillation as well as other features of the pressure power spectrum have been modeled and the agreement with experimental results proves that the model is able to describe the physics of the unsteady reacting flow in the combustor with a high degree of accuracy.

Results are being presented in the form of a comparison between the CFD solution and experimental data. The premixed methane–air mixture enters the combustor with a flow rate of $120\,\mathrm{cm}^3/\mathrm{s}$ and equivalence ratio (ϕ) of 1.0. The incoming temperature of the mixture is 300 K. The unsteady pressure fluctuations were recorded at two locations—5 cm upstream and 5 cm downstream of the honeycomb. Unlike the simulation carried out by Cho et al. [16], this simulation does not use the 'instability triggering method' [23] to simulate the coupling mechanism between unsteady heat release rate and acoustics. Instead, the natural growth of the instability is captured by the numerical model.

4.1. Dynamic characteristics of the combustor

To capture the dynamic characteristics of the combustor, time-accurate integration of the conservation equations was carried out. Two different regimes are present in the unsteady simulation: (1) the exponential growth of the instability; (2) subsequent limit-cycle behavior. The pressure anti-node at the inlet and the node at the exit of the combustor can be seen in Fig. 8. The figure shows instantaneous axial pressure distribution along the centerline of the combustor. For the present closed–open tube combustor, the second acoustic mode is excited and exhibits a limit-cycle. The shape of the curve indicates a three-quarter mode shape. The pressure maximum occurs downstream of the honeycomb (at the 1 m location), which matches the theoretical pressure maximum location for a three-quarter wave form.

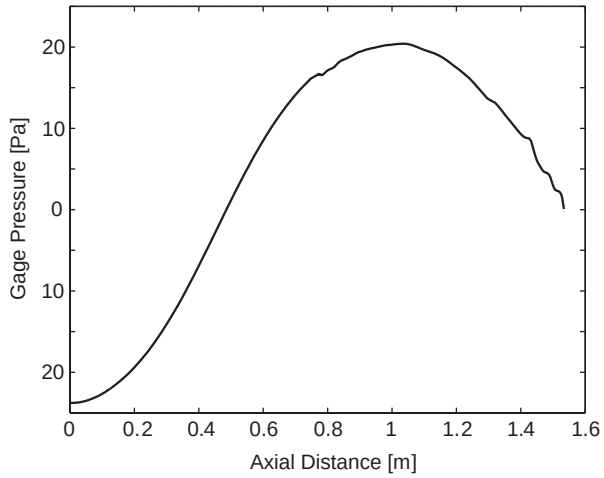

Fig. 8. Pressure mode shape for the second acoustical mode of the tube combustor.

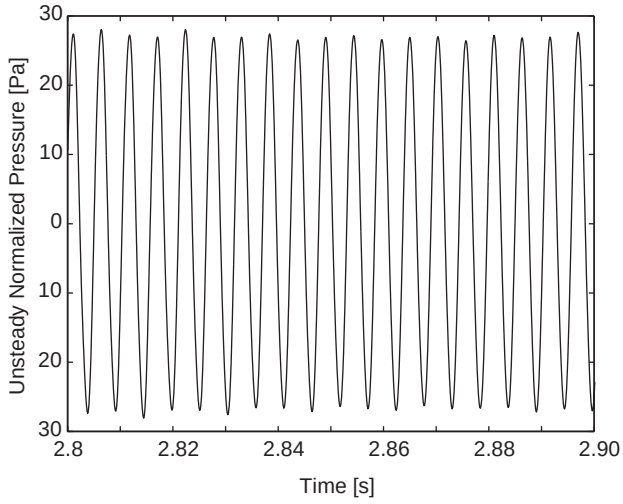

Fig. 9. Growth of unsteady pressure measured 5 cm downstream of the honeycomb.

The following sections document the observations in the two regimes—the growth of instability regime and the subsequent limit-cycle behavior.

4.1.1. Growth of instability

The instability growth mechanism is characterized by increasing oscillations of pressure inside the combustor. This growth (seen in Fig. 9) is captured by the computational model. It can be observed that at approximately 0.2 s after the time integration was initialized, the pressure starts oscillating. This oscillation grows till about 0.4 s and then saturates to a limit-cycle behavior. Once the limit-cycle amplitude is reached, the pressure has a fixed mean amplitude of oscillation. The

amplitude is only affected by the other dynamics of the combustor—the effect of the pulsating instability, for example.

4.1.2. Limit-cycle and pressure power spectrum

The limit-cycle behavior of the unsteady pressure inside the combustor can be observed in Fig. 10.

The pressure power spectrum (Fig. 11) shows that the following characteristics of the acoustic signature of the combustor have been captured:

- The fundamental frequency corresponding to the three-quarter mode of the combustor has been captured to be 190 Hz. The magnitude of the peak is approximately 178 dB.
- The first four harmonics of the fundamental frequency are visible at 380, 570, 760 and 950 Hz.
- A peak at around 70 Hz can also be observed.

Although the fundamental frequency at which the instability occurs and its harmonics have been predicted, two major features of the power spectrum which were observed in the experimental studies have not been captured by the computational model. It will be shown in the following section that averaging methods applied to the data make the pulsating instability mechanism visible in the spectrum, while the subharmonic instability that was observed in experiments to happen around 90 Hz is not predicted by the model. Specifically, the model was unable to capture the mode shapes exhibited by the flame observed in the experimental studies. Two alternate and independent reasons can be given as an explanation of the peak observed at 70 Hz in the computational study:

(1) Using the finite element method to calculate the modes of the combustor for cold flow, Nord [6] showed that the first mode of the combustor existed at 63 Hz and the second occurred at 166 Hz. The second acoustic mode (the 3/4 mode) gets excited for the reacting flow in the combustor and is observed at 182 Hz in the experiments. It can be assumed that the

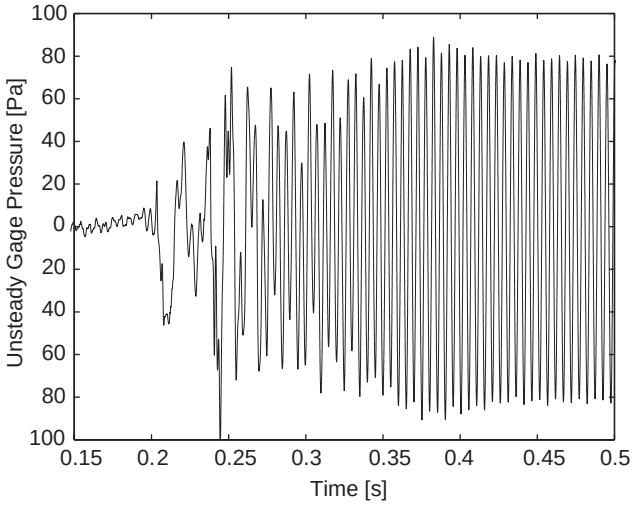

Fig. 10. Time trace of the unsteady pressure oscillation in the combustor.

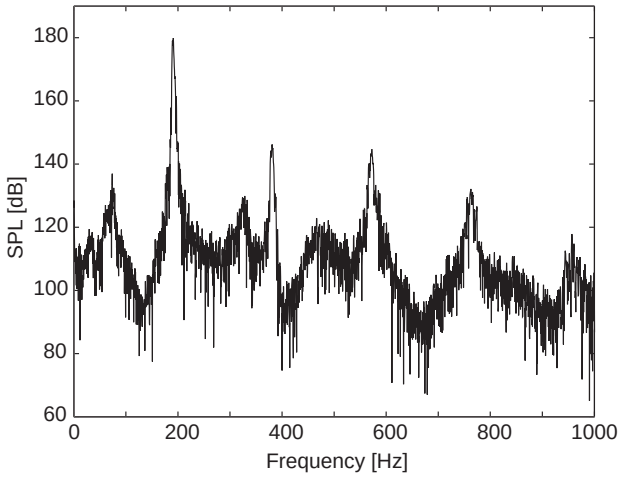

Fig. 11. Pressure power spectrum showing limit-cycle (—, computed).

computational results over-predict the first acoustic mode of the system as compared to the damped mode seen in experimental results. The frequency at which the first mode is predicted (70 Hz) is higher than the 63 Hz cold acoustic calculations because of the presence of higher temperatures in the combustor (hot acoustics).

(2) An alternate explanation for the 70 Hz peak can be that the model has been able to predict the subharmonic peak but tends to under predict the frequency by 20 Hz. In the experimental studies, a question was raised as to whether the subharmonic instability is dependent on the limit-cycle amplitude or the limit-cycle frequency. It was suggested that the flame sheet has preferred frequencies which can be seen as resonances of the flame and are observed as the subharmonic peak in the pressure power spectrum. These resonances, mentioned in Section 2.2.1, were seen in the experiments as non-axisymmetric (three-dimensional) mode shapes exhibited by the flame. The failure to correctly capture such a 'preferred' frequency by the CFD model may result in the under prediction of the subharmonic instability.

Another explanation can be that the subharmonic response of the flame is not captured by the two-dimensional CFD model because of the inherent three dimensionality of the mode shapes exhibited by the flame. Therefore, it can be argued that the second explanation is probably not true and the 70 Hz peak is the first mode of the combustor which is over predicted.

4.1.3. The pulsating instability

A closer look at the limit-cycle pressure oscillation (Fig. 10) reveals the presence of frequencies other than the fundamental. Included in these frequencies, along with the harmonics of the fundamental (at 190 Hz), is the pulsating instability (mentioned in Section 2) which results in amplitude modulation of the fundamental frequency and the harmonics and is visible in the form of sidebands on the frequency peaks. In Fig. 11, the pressure power spectrum shown is obtained without averaging the data. Upon using averaging methods available in MATLAB, the pulsating

instability occurring in the combustor can be captured. A Hanning window method was used to average the data (3.5 s of data) and a sliding window was applied. Fig. 12 shows the pressure power spectrum obtained with the averaging techniques implemented. Sidebands on the fundamental frequency and the pulsating instability are also shown in the figure. The pulsating instability can be seen around the low frequency region and is observed at 24 Hz. The sideband locations on the fundamental frequency are 190 ± 24 Hz.

4.1.4. Comparison with experimental results

The computed pressure power spectrum for $\phi = 1.0$ and $Q = 120\,\mathrm{cm}^3/\mathrm{s}$ is compared with the power spectrum generated from experimental results. Fig. 13 presents the computed and

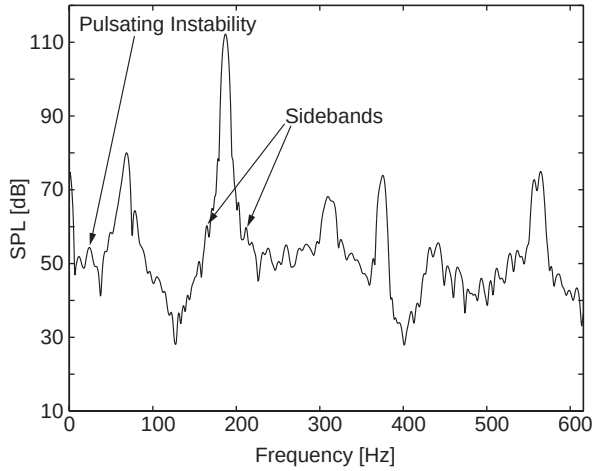

Fig. 12. Amplitude modulation and the subsonic instability.

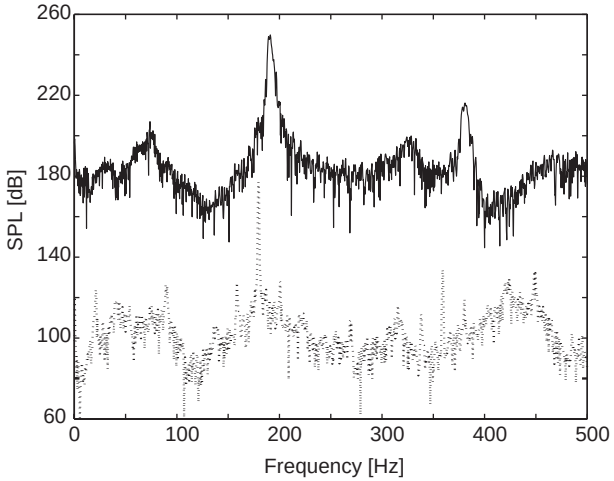

Fig. 13. Comparison between computed results and experimental results (⋯, experiment; —, computed + 70 dB).

Table 1
Comparison between simulation and experimental data

	Simulation	Experiment
Fundamental frequency (Hz)	190	182
Fundamental frequency amplitude (dB)	178	177
Pulsating instability frequency (Hz)	24	21

experimental data on the same plot. The computed data curve has been staggered from the experimental data curve by 70 dB so that the two curves can be compared easily. The thermoacoustic instability is predicted to occur at 190 Hz as compared to 182 Hz measured in the experiments. The computed magnitude is 178 dB whereas the experimental value calculated is 177 dB. As can be seen in Fig. 13, the subharmonic frequency (91 Hz, half of the fundamental 182 Hz) is visible in the experimental pressure power spectrum. The 70 Hz peak that can be observed in the computed power spectrum cannot be the under predicted subharmonic frequency (as discussed in Section 4.1.2). It can therefore be hypothesized that the 70 Hz frequency is indeed the first mode of the combustor. The difference between the predicted cold-acoustics value of 63 Hz and the computed 70 Hz hot-acoustics value is expected.

5. Summary and conclusions

A numerical simulation of reacting flow in the combustor was successfully carried out for $\phi = 1.0$ and $Q = 120\,\mathrm{cm}^3/\mathrm{s}$. The objective of capturing the thermoacoustic instability in the combustor was achieved and the acoustic signature obtained from the experimental investigation was replicated by the computed results. Unsteady growth of pressure oscillation was observed in the simulation indicating that the numerical model was able to capture the limit-cycle phenomena which occurs in the Rijke tube combustor.

The fundamental instability frequency is predicted close to the second mode of the acoustic system and matches well with the experimentally obtained value. Other features of the measured pressure power spectrum have been captured accurately. The effect of this instability is observed on the fundamental frequency as well as the harmonics in the form of sidebands due to amplitude modulation. Table 1 shows the comparison between computed values and experimental data. Further investigation has been carried out to study the effect of acoustics on the flat flame heat release rate response. The work carried out will be included in an upcoming article.

Acknowledgements

The authors wish to acknowledge the support of this work as part of an AGTSR contract, No. 98-01-SP065. Project monitors were Dr. Daniel B. Fant and Dr. Richard A. Wenglarz.

References

[1] R.L. Raun, M.W. Beckstead, J.C. Finlinson, K.P. Brooks, A review of Rijke tubes, Rijke burners and related devices, *Progress in Energy and Combustion Sciences* 19 (1993) 313–364.
[2] M.M. Friedlander, T.J.B. Smith, Experiments on the Rijke tube phenomenon, *Journal of the Acoustical Society of America* 36 (1964) 17.
[3] N.C. Pelcé, One-dimensional model for the Rijke tube, *Journal of Fluid Mechanics* 202 (1989) 83–96.
[4] D.M. Nark, J.C. Hardin, The Rijke tube as an initial value problem, AIAA-97-1626-CP, 1997, pp. 325–333.
[5] H.-G. Yoon, J. Peddieson Jr., K.R. Purdy, Mathematical modeling of a generalized Rijke tube, *International Journal of Engineering Science* 36 (1998) 1235–1264.
[6] L. Nord, A Thermoacoustic Characterization of a Rijke Tube Combustor, Master's Thesis, Virginia Tech, 2000.
[7] J.W.S. Rayleigh, *The Theory of Sound*, vol. 2, Dover Publications, New York, 1945 (re-issue).
[8] H. Yan, Numerical simulation and experimental investigation of self-excited oscillating flows in Rijke tubes, in: *Proceedings of the 33rd National Heat Transfer Conference*, Albuquerque, NM, August 15–17, 1999.
[9] T. Ishii, E. Hihara, T. Saito, Numerical analysis on heat-induced vibration of air column, *JSME International Journal* 41 (3) (1998) 674–681.
[10] B. Entezam, J. Majdalani, W.K. van Moorhem, Modeling of a Rijke-tube pulse combustor using computational fluid dynamics, AIAA Paper 97-2718, Seattle, WA, July 1997.
[11] *Flow 3D Solvers*, Flow Science Incorporated, Los Alamos, NM, USA.
[12] B. Entezam, J. Majdalani, W.K. van Moorhem, A novel investigation of the thermoacoustic field inside a Rijke tube, in: *Seventh AIAA/ASME Joint Thermophysics and Heat Transfer Conference*, Albuquerque, NM, June 15–18, 1998.
[13] C.-C. Hantschk, D. Vortmeyer, Numerical simulation of self-excited thermoacoustic instabilities in a Rijke tube, *Journal of Sound and Vibration* 277 (3) (1999) 511–522.
[14] *FLUENT Solvers*, Fluent Incorporated, Lebanon, NH, USA.
[15] C.-C. Hantschk, D. Vortmeyer, Numerical simulation of unsteady interactions between flow, heat conduction and acoustics within a Rijke tube, *Chemical Engineering and Technology* 23 (9) (2000) 758–763.
[16] C. Sangyeon, K. Jaeheon, L. Soogab, Characteristics of thermoacoustic oscillation in a ducted flame burner, in: *Proceedings of the 36th Aerospace Sciences Meeting and Exhibit*, Reno, NV, January 12–15, 1998.
[17] A.A. Amsden, P.J. O'Rourke, T.D. Butler, KIVA-II: a computer program for chemically reactive flows with sprays, Los Alamos Scientific Laboratory Reports, 1989.
[18] W.R. Saunders, L. Nord, C.A. Fanin, H. Ximing, W.T. Baumann, U. Vandsburger, V.K. Khanna, L.C. Haber, B. Eisenhower, S. Liljenberg, Diagnostics and modeling of acoustic signatures in a tube combustor, in: *Proceedings of the Sixth International Conference of Sound and Vibration*, Copenhagen, Denmark, July 1999.
[19] G.H. Markstein, *Nonsteady Flame Propagation*, The Macmillan Company, Pergamon Press, New York, 1964.
[20] G.H. Margolis, Nonsteady flame propagation, *Combustion Science and Technology* 22 (1980) 143–169.
[21] Fluent Inc., *Fluent 5 User's Guide*, 2000.
[22] C.K. Westbrook, F.L. Dryer, Chemical kinetic modeling of hydrocarbon combustion, *Progress in Energy and Combustion Science* 10 (1984) 1–57.
[23] M. Habiballah, I. Dubois, Numerical analysis of engine instability, liquid rocket engine combustion instability, *Progress in Astronautics and Aeronautics* 169 (1995) 475–502.